Synchronizing spatiotemporal chaos in coupled map lattices via active-passive decomposition

Wang Jinlan,[1] Chen Guangzhi,[1] Qin Tuanfa,[2] Ni Wansun,[3] and Wang Xuming[1]
[1]*Department of Physics, Guangxi University, Nanning 530004, People's Republic of China*
[2]*College of Computer and Information Engineering, Guangxi University, Nanning 530004, People's Republic of China*
[3]*Institute of Acoustics and State Key Laboratory of Modern Acoustics, Nanjing University, Nanjing 210093, People's Republic of China*
(Received 22 October 1997; revised manuscript received 16 April 1998)

We realize spatiotemporal chaotic synchronization in coupled map lattices with active-passive decomposition synchronization schemes [K. Kocarev and U. Parlitz, Phys. Rev. Lett. **74**, 5028 (1995)]. The synchronization conditions and the synchronization ranges are given in theory and demonstrated in numerical experiments. The further relation between the coupling strength and the synchronization efficiency is investigated numerically. This method offers high security and the signal can be recovered exactly. These properties make the method potentially useful in secure communication.
[S1063-651X(98)01509-8]

PACS number(s): 05.45.+b

I. INTRODUCTION

Synchronization of chaos seems impossible because of its sensitive dependence on initial conditions. However, since the pioneering work of Pecora and Carroll [1], synchronization in chaotic systems and its applications, particularly in communication, have been extensively investigated and some progress has been made [2–10].

Pyragas adapted the continuous linear feedback method to control and synchronize chaos [2] and De Soisa Vieira and Lichtenberg further generalized it to mappings by feeding back the nonlinear mapping signal [11]. As a generalization of the Pecora-Carroll method, Kocarev and Parlitz [12] suggest a different approach, *active-passive decomposition* (APD). This method can realize perfect synchronization with one or more drive variables and the drive variables can be chosen freely. Moreover, when it is applied to communication, the signal can be recovered exactly. These properties make the method potentially useful in secure communication [12–14].

On the basis of [11], we generalize the APD method to mappings. The purpose of this paper is to utilize the APD method to synchronize the spatiotemporal chaos in coupled map lattices [15] in the case of one-way coupling and two-way coupling and to investigate its potential applications in communication. Spatiotemporal chaos makes the signal more unpredictable and more complicated, which make it more difficult to extract information from an intercepted signal.

II. APD SYNCHRONIZATION SCHEME IN A ONE-DIMENSIONAL MAP

We consider the logistic map

$$x_{n+1}=f(x_n)=4ax_n(1-x_n). \tag{1}$$

The nonlinear autonomous system (1) can formally be written as a nonautonomous system with the APD method,

$$x_{n+1}=px_n+g_n, \tag{2}$$

$$g_n=4ax_n(1-x_n)-px_n. \tag{3}$$

Then a duplicated system (2) with the same driving g_n is

$$y_{n+1}=py_n+g_n, \tag{4}$$

so we can get the difference equation $\Delta x_{n+1}=x_{n+1}-y_{n+1}$:

$$\Delta x_{n+1}=p\Delta x_n. \tag{5}$$

Obviously, if $|p|<1$, the sequence $\{\Delta x_n\}$ is convergent. The absolute difference between the variables decreases to zero as n (time) increases, indicating the existence of perfect synchronization between systems (2) and (4).

The above synchronization scheme may be used in secure communication. We consider systems (2) and (4) as the transmitter and the receiver, respectively, and the drive variable g_n as the signal of the transmitter sending and the receiver receiving, including the chaotic signal and the information signal S_i. Generally, the system parameters (here a) should make the system chaotic. Assuming that R_i is the recovered signal in the receiver, from Eqs. (3) and (4) we have

$$R_i=g_n-4ay_n(1-y_n)+py_n. \tag{6}$$

When the transmitter and the receiver synchronize, $y_n \to x_n$; therefore, $R_i=S_i$. On the contrary, if the synchronization is lost, then $y_n \neq x_n$; thus $R_i \neq S_i$ and the original signal can not be recovered.

From the above discussion, it is not difficult to see that the APD scheme can achieve full synchronization with identical dynamics and the signal can be recovered exactly. Further, the freedom of choices of g_n broadens the applications in practice.

III. THEORETICAL AND NUMERICAL ANALYSIS OF THE SPATIOTEMPORAL CHAOS SYNCHRONIZATION OF COUPLED MAP LATTICES

Consider the symmetrical coupled map lattice (CML) model

$$x_{n+1}(i)=\epsilon_1 f(x_n(i+1))+\epsilon_2 f(x_n(i-1)) +(1-\epsilon_1-\epsilon_2)f(x_n(i)), \tag{7}$$

where $f(x_n)$ is some nonlinear discrete map that can sustain chaotic motion, x_n is the state variable, $i=1,2,...,L$ is the lattice site index, n is the time index, and ϵ_1 and ϵ_2 are the coupling constants. To simplify the problem, we suppose that Eq. (7) has a periodic boundary condition $x_n(i+L)=x_n(i)$, with L being the system size. In the following we will synchronize spatiotemporal chaos in one-way coupled map lattices (OCMLs) and two-way coupled map lattices (TCMLs) via the APD synchronization scheme.

A. Example 1: The OCML system with $L=3$

For this case, Eq. (7) is rewritten as

$$x_{n+1}(i)=\epsilon_i f(x_n(i+1))+(1-\epsilon_i)f(x_n(i)), \quad i=1,2,3. \tag{8}$$

Based on the APD synchronization scheme, we construct the synchronized systems as the transmitter-receiver systems as follows: For the transmitter

$$\begin{aligned} x_{n+1}(1)&=(1-\epsilon_1)f(x_n(1))+g_n,\\ x_{n+1}(2)&=\epsilon_2 f(x_n(3))+(1-\epsilon_2)f(x_n(2)),\\ x_{n+1}(3)&=\epsilon_3 f(x_n(1))+(1-\epsilon_3)f(x_n(3)); \end{aligned} \tag{9}$$

the transmitted signal

$$g_n=\epsilon_1 f(x_n(2))+S_i; \tag{10}$$

the receiver

$$\begin{aligned} y_{n+1}(1)&=(1-\epsilon_1)f(y_n(1))+g_n,\\ y_{n+1}(2)&=\epsilon_2 f(y_n(3))+(1-\epsilon_2)f(y_n(2)),\\ y_{n+1}(3)&=\epsilon_3 f(y_n(1))+(1-\epsilon_3)f(y_n(3)); \end{aligned} \tag{11}$$

and the recovered signal

$$R_i=g_n-\epsilon_1 f(x_n(2)), \tag{12}$$

where S_i is the information signal and $\epsilon_i (i=1,2,3)$ the coupling strength. We take the tent map

$$x_{n+1}=f(x_n)=\begin{cases} 2ax_n, & 0<x_n\leqslant 0.5\\ 2a(1-x_n), & 0.5<x_n<1 \end{cases} \tag{13}$$

as the nonlinear function to conduct a theoretical analysis and numerical experiments. We know that the tent map is fully chaotic in the range $a\in(0.715,1)$; therefore, we can choose the parameter $a\in(0.715,1)$ to guarantee that both systems are chaotic. Given $x_n,y_n\in(0,0.5)$, then $f(x_n)=2ax_n$. From Eqs. (9) and (11) we get

$$\Delta x_{n+1}(i)=\mathbf{A}\Delta x_n(i), \tag{14}$$

where $\mathbf{A}$ is a 3×3 Jacobian matrix

$$\mathbf{A}=\begin{pmatrix} 2a(1-\epsilon_1) & 0 & 0\\ 0 & 2a(1-\epsilon_2) & 2a\epsilon_2\\ 2a\epsilon_3 & 0 & 2a(1-\epsilon_3) \end{pmatrix}.$$

The eigenvalues of the Jacobian matrix are

$$\lambda_i=2a(1-\epsilon_i), \quad i=1,2,3. \tag{15}$$

If

$$|2a(1-\epsilon_i)|<1 \quad \text{or} \quad 1-\frac{1}{2a}<\epsilon_i<1+\frac{1}{2a}, \tag{16}$$

the sequence $\{\Delta x_n(i)\}$ is convergent. As time elapses, $\Delta x_{n+1}(i)=|x_{n+1}(i)-y_{n+1}(i)|$ tends to zero. Systems (9) and (11) are synchronized perfectly.

When $x_n,y_n\in(0.5,1)$, a similar discussion gets the same results. Moreover, coupling strength should satisfy $\epsilon_i<1$ to guarantee the stability of the maps. Therefore, the synchronization ranges of the coupling strength are $1-1/2a<\epsilon_i<1$.

Numerical experiments ($a=0.785$) show that systems (9) and (11) are perfectly synchronized and the signals are recovered exactly [Fig. 1(b)] when $\epsilon_i\in(0.363,1)$. The transmitted signal [Fig. 1(a)] is chaotic. No synchronization can be achieved with $\epsilon_i<0.363$. The synchronization time as a function of the coupling strength is also studied and shown in Fig. 2(a). It is clear that the stronger the coupling, the shorter the synchronization time. We give a heuristic explanation of this property. If the coupling strength is sufficiently large ($\epsilon_i<1$), the lattices behave almost like a single lattice and it is easy to synchronize. If the coupling is small, the connection between lattice elements become weak and the drive signal needs a long time to entrain the receiver system to the transmitter. If the coupling is too small, they behave almost independently and the synchronization conditions are unsatisfied. For inhomogeneous coupling, as long as $\epsilon_i\in(0.363,1)$, the synchronization is still obtained. Figure 2(b) plots the curve of n versus ϵ_2 with $\epsilon_1=\epsilon_3=0.5$ as Fig. 2(a).

When the parameters of the two systems are mismatched, slightly different coupling strengths lead to desynchronization and the recovered signal has a large error. Figure 3 shows the results with $\epsilon_i=0.5$ and $\epsilon_i'=0.505$. The system is desynchronized, so the synchronization via the APD scheme is sensitive to the system parameters.

The above discussion is generalized to many CML's ($L>3$). Figure 4(a) depicts the same diagram as in Fig. 1(b) but with $L=60$, $\epsilon_i=0.5$, and $S_i=0.2\sin(0.2\pi t)$. Numerical experiments show that the synchronization ranges become smaller [$L=60$ and $\epsilon_i\in(0.368,0.854)$] and the synchronization time needs to be longer with L increasing. Figure 4(b) plots the relation curve of the synchronization time (n) and the system size (L). In this diagram, we average n over 20 realizations with different initial conditions (varying ϵ from

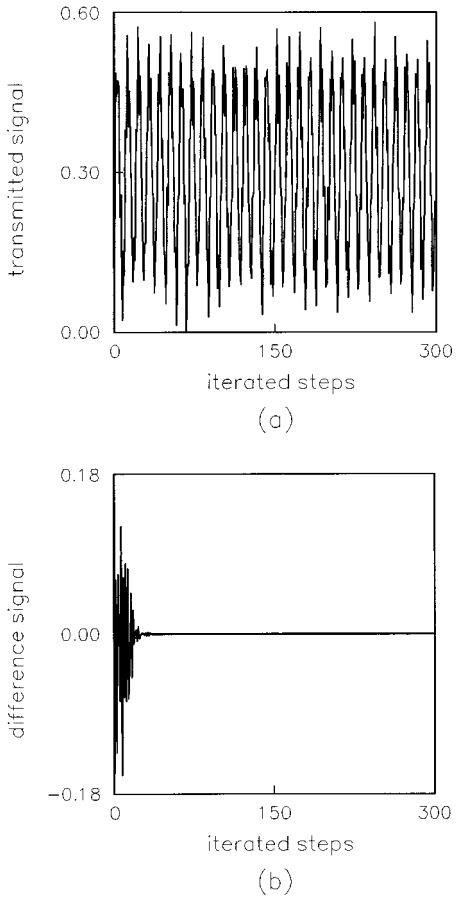

FIG. 1. The APD method in the OCML is applied to secure communication with $L=3$, $a=0.785$, $\epsilon_i=0.5$, and $S_i=0.2\sin(0.2\pi t)$: (a) the transmitted drive signal $g_n=\epsilon_1 f(x_n(2))+S_i$ and (b) perfect synchronization. The difference signal S_i-R_i is plotted versus time (iterated steps n) for identical parameters of the transmitter and receiver.

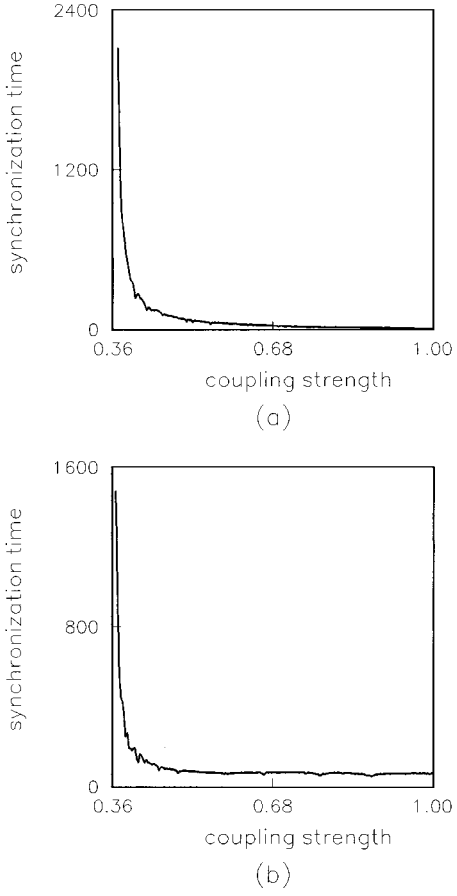

FIG. 2. Relation of the synchronization time versus the coupling strength with the accuracy of $|S_i-R_i|$ being 10^{-6}: (a) homogeneous coupling and (b) inhomogeneous coupling with $\epsilon_1=\epsilon_3=0.5$.

0.4 to 0.5 with the interval 0.005) to smooth small fluctuations as [16]. Obviously, their relation is approximated by

$$n\propto L. \tag{17}$$

This may be explained as follows: The global synchronization in many CMLs is attained by transferring synchronization from one lattice element to another, so the larger the system size, the more time needed for the drive signal to entrain all the lattice elements of the receiver to those of the transmitter.

B. Example 2: TCMLs with $L=3$

In this case Eq. (7) becomes

$$x_{n+1}(i)=(1-\epsilon)f(x_n(i))+\frac{\epsilon}{2}[f(x_n(i+1))+f(x_n(i-1))],\quad i=1,2,3. \tag{18}$$

Here we assume that the coupling is homogeneous. We conduct a theoretical and numerical analysis as in example 1. For the transmitter

$$x_{n+1}(1)=(1-\epsilon)f(x_n(1))+g_n,$$

$$x_{n+1}(2)=(1-\epsilon)f(x_n(2))+\frac{\epsilon}{2}[f(x_n(1))+f(x_n(3))], \tag{19}$$

$$x_{n+1}(3)=(1-\epsilon)f(x_n(3))+\frac{\epsilon}{2}[f(x_n(2))+f(x_n(1))];$$

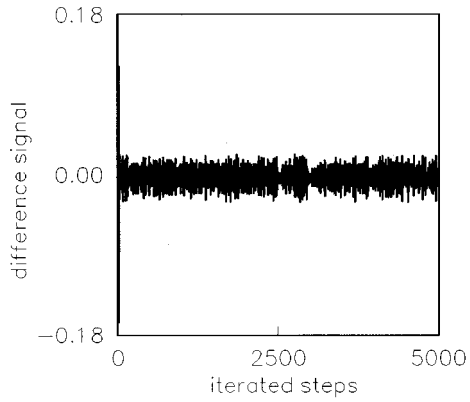

FIG. 3. Nonsynchronization as in Fig. 1(b). A small discrepancy of the coupling strength (in the transmitter $\epsilon_i=0.5$, in the receiver $\epsilon_i'=0.505$) leads to a large difference signal.

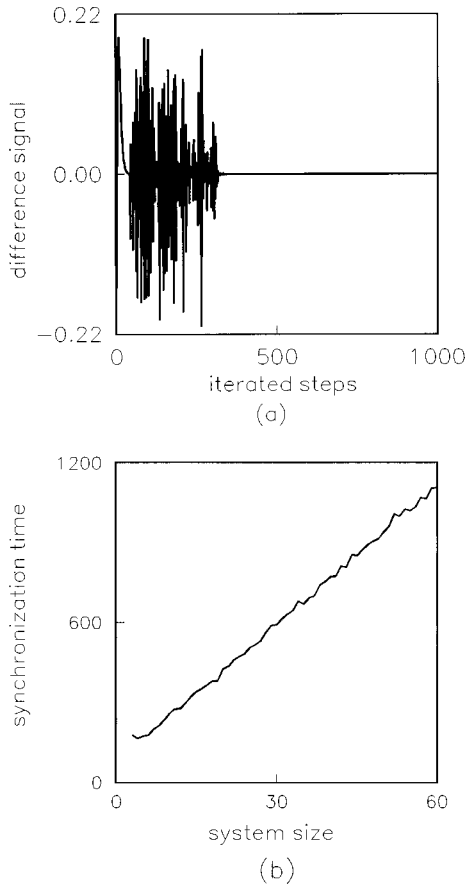

FIG. 4. Synchronization for many CMLs ($L=60$). The rest of the conditions are the same as in Fig. 1: (a) difference signal versus time and (b) synchronization time as a function of the system size L with the accuracy of the difference signal being 10^{-6}.

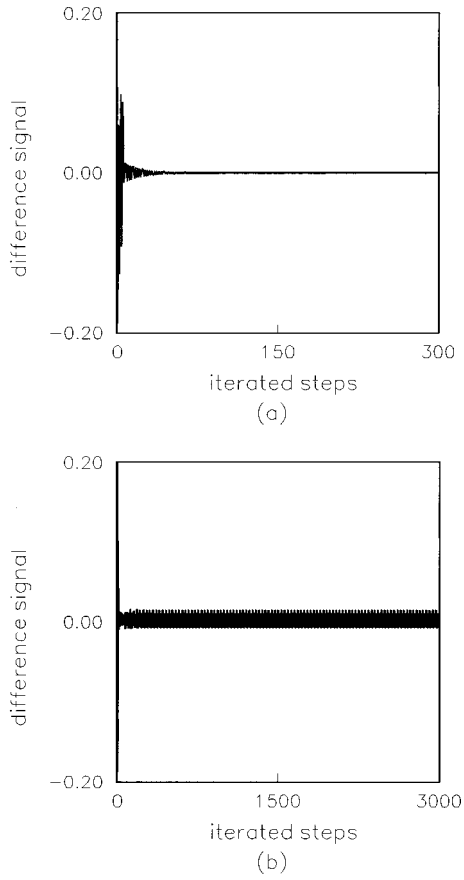

FIG. 5. Synchronization in two-way coupling as in Fig. 1: (a) synchronization with identical parameters $\epsilon=\epsilon'=0.8$ and (b) nonsynchronization for the mismatched parameters $\epsilon=0.8$, and $\epsilon'=0.805$.

the transmitted signal

$$g_n=\frac{\epsilon}{2}[f(x_n(2))+f(x_n(3))]+S_i; \tag{20}$$

the receiver

$$y_{n+1}(1)=(1-\epsilon)f(y_n(1))+g_n,$$

$$y_{n+1}(2)=(1-\epsilon)f(y_n(2))+\frac{\epsilon}{2}[f(y_n(1))+f(y_n(3))], \tag{21}$$

$$y_{n+1}(3)=(1-\epsilon)f(y_n(3))+\frac{\epsilon}{2}[f(y_n(2))+f(y_n(1))];$$

and the recovered signal

$$R_i=g_n-\frac{\epsilon}{2}[f(x_n(2))+f(x_n(3))]. \tag{22}$$

When $x_n, y_n \in (0,0.5)$ we have

$$\begin{pmatrix}\Delta x_{n+1}(1)\\ \Delta x_{n+1}(2)\\ \Delta x_{n+1}(3)\end{pmatrix}=\begin{pmatrix}2a(1-\epsilon) & 0 & 0\\ a\epsilon & 2a(1-\epsilon) & a\epsilon\\ a\epsilon & a\epsilon & 2a(1-\epsilon)\end{pmatrix}\times\begin{pmatrix}\Delta x_n(1)\\ \Delta x_n(2)\\ \Delta x_n(3)\end{pmatrix}. \tag{23}$$

The eigenvalues are obtained using

$$\lambda_1=2a-a\epsilon, \quad \lambda_2=2a-2a\epsilon, \quad \lambda_3=2a-3a\epsilon. \tag{24}$$

The synchronization conditions are $|\lambda_i|<1$ so the range is $\epsilon\in(2-1/a,1)$. For $x_n, y_n \in (0.5,1)$, the results are the same. Therefore, the synchronization range is $\epsilon\in(2-1/a,1)$.

Numerical experiments verify this, for example, $a=0.785$ and $\epsilon\in(0.726,1)$. Moreover, the coupling strength has an effect on synchronization that is similar to that in one-way coupling. Figures 5(a) and 5(b) depict the synchronization and nonsynchronization results, respectively, corresponding to identical parameters $\epsilon=\epsilon'=0.8$ and mismatched parameters $\epsilon=0.8$ and $\epsilon'=0.805$. However, it is very difficult to synchronize with larger TCMLs ($L>3$). For example, for $L=4$, synchronization can be achieved for only some coupling strengths. Even though the system's Jacobian factorizes very nicely in the OCMLs system and the Lyapunov exponents for synchronization can be related to

the Lyapunov exponents of the individual maps, this does not happen for the two-way coupled system. The dramatic differences can be seen as the number of coupled maps increases from 3 to 4.

It is worth pointing out that in either one-way or two-way coupling, the information signal has relatively less restriction than for the Pecora-Carroll scheme. The strength and frequency of the signal have little effect on the synchronization efficiency, but a very large strength may lead to data overflowing.

IV. CONCLUSION

We have realized spatiotemporal chaos synchronization in CMLs via the APD synchronization scheme and investigated its potential applications in communication. We have shown that the APD scheme can realize perfect spatiotemporal chaotic synchronization by only using a one-dimensional drive signal and the information signal can be recovered exactly. The synchronization ranges have been given in theory and the relation between the synchronization and the coupling strength has been studied in numerical experiments. We have further generalized the APD method to many OCML spatiotemporal chaotic systems and discussed the relation between the synchronization time and the system size. We have also indicated that mismatched parameters between the transmitter and the receiver systems lead to desynchronization and the signal cannot be recovered. Moreover, the transmitter, the receiver, and the driving signal are all spatiotemporal chaotic, which improves the encrypting efficiency. It is worth noting that the discrete model is amenable for implementation on both software and hardware. These advantages make it very promising in secure communication applications.

ACKNOWLEDGMENT

The work was supported by the National Natural Science Foundation of China.

[1] L. M. Pecora and T. L. Carroll, Phys. Rev. Lett. **64**, 821 (1990); Phys. Rev. A **44**, 2374 (1991).
[2] K. Pyragas, Phys. Lett. A **170**, 421 (1992); **181**, 201 (1993).
[3] T. C. Newell, P. M. Alsing, A. Gavrielides, and V. Kovanis, Phys. Rev. Lett. **72**, 1647 (1994); Phys. Rev. E **49**, 313 (1994).
[4] A. Maritan and J. R. Banavar, Phys. Rev. Lett. **72**, 1451 (1994).
[5] T. L. Carroll and L. M. Pecora, IEEE Trans. Circuits Syst. **40**, 646 (1990).
[6] M. De Sousa Vieira, A. J. Lichtenberg, and M. A. Lieberman, Int. J. Bifurcation Chaos Appl. Sci. Eng. **1**, 701 (1991).
[7] T. Endo and L. O. Chua, Int. J. Bifurcation Chaos Appl. Sci. Eng. **2**, 61 (1992).
[8] L. O. Chua, L. Kocarev, K. Eckert, and M. Itoh, Int. J. Bifurcation Chaos Appl. Sci. Eng. **2**, 705 (1992).
[9] K. M. Cuomo and A. V. Oppenheim, Phys. Rev. Lett. **71**, 65 (1993).
[10] L. Kocarev, K. S. Halle, K. Echert, and L. O. Chua, Int. J. Bifurcation Chaos Appl. Sci. Eng. **2**, 709 (1992).
[11] M. De Soisa Vieira and A. J. Lichtenberg, Phys. Rev. E **54**, 1200 (1996).
[12] L. Kocarev and U. Parlitz, Phys. Rev. Lett. **74**, 5028 (1995).
[13] L. Kocarev, U. Parlitz, and T. Stojanovski, Phys. Lett. A **217**, 280 (1996).
[14] U. Parlitz, L. Kocarev, T. Stojanovski, and H. Preckel, Phys. Rev. E **53**, 4351 (1996).
[15] Gang Hu, Zhilin Qu, and Kaifen He, Int. J. Bifurcation Chaos Appl. Sci. Eng. **5**, 901 (1995).
[16] M. De Soisa Vieira, A. J. Lichtenberg, and M. A. Lieberman, Int. J. Bifurcation Chaos Appl. Sci. Eng. **4**, 1563 (1994).